IEEE Access
Multidisciplinary | Rapid Review | Open Access Journal

- Date of publication xxxx 00, 0000, date of current version xxxx 00, 0000.

Digital Object Identifier 10.1109/ACCESS.2022.Doi Number

Harmonic Distortion Indices for Experimental Characterisation of Variable Frequency Drives

Angel Arranz-Gimon[1], Daniel Morinigo-Sotelo[2], Member, IEEE, Angel Zorita-Lamadrid[2], and Oscar Duque-Perez[2]

[1]Department of Electronic Technology, Universidad de Valladolid, Paseo Prado de la Magdalena 3-5, E-47011 Valladolid, Spain
[2]Research Group ADIRE, Institute of Advanced Production Technologies, Universidad de Valladolid, Paseo del Cauce 59, E-47011 Valladolid, Spain

Corresponding author: Daniel Morinigo-Sotelo (e-mail: daniel.morinigo@uva.es).

This work was supported in part by the Universidad de Valladolid.

ABSTRACT Frequency converters controlling electric motors are widely used as they increase the functionality of the equipment and improve energy efficiency. However, it is inevitable that the quality of the power delivered to the motor does not have the same characteristics as when it is supplied from the mains. Due to the impact of the power quality on the operation of the motor and even on its possible diagnosis, it is desirable to characterise the power quality, preferably by means of rates or indices that reflect the quality as completely as possible. However, the rates specified in the standards and in the literature are designed to characterise the quality delivered from the grid and are not well adjusted to the features of the signal at the output of the converter with a high interharmonic and harmonic content at high and low frequencies, and with variable fundamental frequencies. For this reason, this work proposes a set of distortion rates and the appropriate procedures for calculating them to reflect as reliably as possible the quality of the energy delivered by the converter to the motor. To verify the validity of the proposal, several practical examples are presented with induction motors fed from different frequency converters.

INDEX TERMS Frequency Grouping, Harmonic Distortion Rates, Induction Motor, Power Quality Indices, Time Aggregation, Variable Frequency Drive (VFD).

ABBREVIATIONS

ASD	Adjustable Speed-Drives
CTN	Altivar-66 drive, with Constant Torque control, in Normal mode
CTS	Altivar-66 drive, with Constant Torque control, in Special mode
f1	Fundamental frequency
FF	Fundamental Factor
HF	High-frequency range, from the end of LF to 20 kHz bandwidth of our measurement system
LF	Low-Frequency range, from the first spectral bar to the 40th Harmonic
MCSA	Motor Current Signature Analysis
PWM	Pulse Width Modulation
s	Motor slip
SCAL	PowerFlex-40 drive, with PWM modulation and Scalar mode control
STFT	Short-Time Fourier Transform
TDC	Total Distortion Content factor
$TH_{\&}IHD_{HF}$	Total Harmonic and Interharmonic Distortion rate for HF
$TH_{\&}IHD_{LF}$	Total Harmonic and Interharmonic Distortion rate for LF
$TH_{\&}IHD_{LFHF}$	Total Harmonic and Interharmonic Distortion rate for LF and HF
$TH_{\&}IHDS_{HF}$	Total Harmonic and InterHarmonic Distortion Subgroup for HF
THD	Total Harmonic Distortion rate for LF
THD(t)	Total Harmonic Distortion rate in real time
THDG	Total Harmonic Distortion Group rate
THDS	Total Harmonic Distortion Subgroup rate
THF_{LF}	Total Harmonic-LF Factor
$TIHD_{LF}$	Total InterHarmonic Distortion rate for LF
$TIHD_{LFHF}$	Total InterHarmonic Distortion rate for LF and HF
$TIHDS_{LF}$	Total InterHarmonic Distortion Subgroup for LF
TnHD	Total nonHarmonic Distortion rate
TnHD(t)	Total nonHarmonic Distortion rate in real time

TNHDF	Total Non-Harmonic-LF Distortion Factor
TWD	Total Waveform Distortion rate
TWD(t)	Total Waveform Distortion rate in real time
VECT	PowerFlex-40 inverter, with PWM modulation and Vector mode control
VFD	Variable Frequency Drive
VTN	Altivar-66 inverter, with Variable Torque control, in Normal mode
VTnL	Altivar-66 inverter, with Variable Torque control, in non-Load mode
Yg,h	Harmonic groups
YH,h	Harmonic bar, multiple of fundamental f_1
Yig,h	Interharmonic groups
Yisg,h	Interharmonic subgroups
Ysg,h	Harmonic subgroups

I. INTRODUCTION

Induction motors are a fundamental element in the operation of many industrial processes, as well as a key element in transportation and other sectors of the economy. In addition to its intrinsic characteristics, the possibility of controlling the speed when a frequency converter powers it has made it a practically indispensable element nowadays. It is a robust and reliable element that performs its task with high efficiency. However, the presence of the frequency converter will affect the characteristics of the motor's power waveform, which, in turn, affects its operation. The harmonic and interharmonic content of the stator current waveform will cause several effects on the stator that can affect its operation, for example, by increasing noise, its efficiency by increasing losses, and the life of the motor [1][2]. Given the importance of the induction motor, it is evident that a correct and timely diagnosis of its condition is of great value. This is a very active field of research in which new proposals to improve the reliability of the diagnosis are continuously being published [3][4]. One of the most widespread techniques and special relevance due to its easy practical applicability is the analysis of the motor power supply current (known as Motor Current Signature Analysis or MCSA) to diagnose its condition [5] [6] [7]. However, it has been found that the diagnosis is strongly influenced by the power supply mode of the motor, depending significantly on whether it is powered directly from the mains or by an inverter, but also on the specific converter used and its mode of operation [8].

Taking into account the previous paragraphs, it is important to know the power quality with which the motor is fed, which leads us to require a correct characterisation of the harmonic content that the frequency converter delivers to the motor, and this information can be used to optimise the control of the power converters to improve the harmonic distortion produced by them [9-11], and thus facilitate the diagnosis and prevention of possible failures in the connected equipment.

In addition to the rates outlined in the power quality standards [12-14], several authors have measured using distortion rates the harmonic contamination generated on the grid side by loads consisting of power converters producing a high harmonic content at low and high frequencies, such as photovoltaic inverters [15-19], wind generators [20,21], electronic car battery chargers [22,23], energy-efficient lighting equipment [24-26], or even Adjustable Speed-Drives (ASD) [27-29]. However, in none of these cases has the harmonic distortion on the other side of the electronic converter been experimentally characterised. Moreover, commercial power quality analysers are optimised to measure on the mains side, whose harmonic content differs from that in the connection between the output of the inverter and the motor.

It must be considered that measuring the inverter output requires special characteristics since controlling the motor speed will imply that the fundamental frequency will be variable and will also present a high harmonic and interharmonic content at both low and high frequencies. Consequently, it is necessary to develop a specific set of distortion rates adapted to the characteristics of the output signals of power electronic converters.

Thus, this work aims to develop a methodology for the harmonic characterisation of frequency inverters based on a set of rates and a procedure for their calculation adapted to the specific characteristics of the output signals of the inverters. This set of rates and the way to process them complements those defined in the standards and in the literature, more prepared for evaluating distortion in network signals, providing features not always available in commercial analysers such as:

- differentiating harmonic and interharmonic components at low frequencies
- measuring separately the total distortion at low and high frequencies
- reaching a more comprehensive range of frequencies than in network signals
- admitting variable fundamental frequencies with what this implies for the synchronisation and the calculation of spectral bars
- normalising these rates considering the peculiarities of the output signals of inverters connected to induction motors with possible faults.

To verify the proposed methodology, tests have been carried out with commercial drives connected to motors, and the variations of each of the rates have been experimentally observed when modifying the different parameters of the drive and the load, as well as possible failures in the motor, proving the validity of the proposed method to harmonically characterize frequency inverters.

The rest of the paper is structured as follows: First, Section II reviews the main basic distortion rates and their limitations for measuring the output of variable frequency drives and studies other rates developed by different authors that improve these limitations. Considering the existing rates and the qualities they must fulfill to measure the inverters output, a set of distortion rates suitable for characterising harmonic

distortion at the output of variable frequency drives is proposed in Section III. Then, in Section IV, the way to process or obtain these rates is detailed, considering the characteristics of the signals to be analysed. Section V then shows and analyses the experimental results obtained by feeding a motor from the mains and frequency inverters with different harmonic contents. Finally, Section VI presents the main conclusions of this work.

II. PROBLEMATICS OF DISTORTION RATES

In this section, the existing distortion rates, both in the standards and proposed in the literature, are reviewed, starting from the qualities that must be met by the rates that allow characterising the quality of the electrical power delivered by the frequency inverters. Their limitations are also analysed.

A. QUALITIES TO BE MET BY THE RATES FOR MEASURING DRIVE SIGNALS

Existing distortion rates are intended to measure signals on the power grid, but to be able to characterise the power quality at the output of inverters, they should have several additional features to improve their performance:

- Since the inverters change frequency to control the motor speed, the output signal frequency is not always 50 or 60 Hz, so measurements for different fundamental frequencies must be supported. The synchronism of these measurements must be readjusted to the fundamental harmonic present in each case to achieve this.
- The frequency groupings that form the distortion rates contain different numbers of spectral bars depending on the value of the fundamental frequency, so these groupings will also have to be adapted.
- The time aggregations applied to the distortion rates must adapt their time to values appropriate to the specific nature of the signals present at the drives' output, taking into account their degree of stationarity.
- A more comprehensive frequency range above the 9000 Hz indicated in the IEC standard 61000-4-30 must be achieved, since the converters have higher switching frequencies and multiples of these frequencies than those usually measured in the power grid.
- The rates should cover different frequency ranges, allowing for the measurement of low and high frequencies separately. This is important considering that, in frequency converters, the limit between low and high frequencies is variable as the fundamental frequency changes.
- Distortion rates should be able to measure harmonics and interharmonics separately at low frequencies. At high frequencies, the total harmonic and interharmonic content is usually measured without separation because harmonics at high frequencies are desynchronised by multiplying the error of the fundamental with respect to the sampling window. Therefore, these high-frequency harmonics act as interharmonics, generating spectral leakage.
- The rates obtained should be normalised, taking into account the characteristics of the signals measured at the drives' output. This will avoid the appearance of continuous and interharmonic components in the denominator, which may produce uncertain results.

B. EXISTING DISTORTION RATES AND LIMITATIONS TO CHARACTERIZE DRIVES

Harmonic distortion can be assessed in two distinct ways [30]. The first method involves measuring each harmonic individually and normalising it by dividing it by the rms value of the fundamental frequency component. The second method, known as distortion rates, provides a global assessment by measuring the rms value of the sum of a set of harmonics, also normalised by the fundamental.

The *Total Harmonic Distortion* rate (*THD*), defined in IEC 61000-4-7 [14] and IEEE 519 [12], is the most basic distortion rate. It evaluates the amplitude of the fundamental frequency versus other low-frequency harmonic-only values of the measured signal [31]. Other basic rates, such as *Total Waveform Distortion* (*TWD*) and *Total nonHarmonic Distortion* (*TnHD*) rate [32], evaluate the entire distortion, including harmonics and interharmonics (*TWD*), or only interharmonics (*TnHD*). More recently, in [33], the real-time harmonic distortion of the analysed signal is evaluated in the time-frequency domain by applying the *Short-Time Fourier Transform* (*STFT*). Thus, the *THD(t)*, *TWD(t)* and *TnHD(t)* indices are obtained, which calculate the *THD*, *TWD* and *TnHD* rates in real-time. However, all these rates evaluate this harmonic distortion but without distinguishing between high and low frequency ranges.

The IEC 61000-4-7 [14] standard is also followed by the IEEE 519 [12] norm. The IEC standard uses the *THD* distortion rate and, in addition, defines two other rates that use the frequency and time groupings to reduce the effects of the non-stationarity of the analysed signal: *Total Harmonic Distortion Group* rate (*THDG*) and *Total Harmonic Distortion Subgroup* rate (*THDS*). With *THDG*, all interharmonics around each harmonic are considered. However, *THDS* only considers the harmonics and their adjacent bands, which are mainly driven by the phase and amplitude variations of the harmonics. These new *THDG* and *THDS* rates complement the existing *THD* rate, which did not assess interharmonics and did not consider signal non-stationarity, although they all measure only low-frequency contents.

While the previous indices have been widely used for the assessment of harmonic distortion, they have certain limitations. With the increasing use of power electronics, the harmonic and interharmonic content and the frequency range to be measured have expanded. As a result, the previous rates show limitations in distinguishing measurements according to their frequency range (low or harmonic frequencies, as

well as supra-harmonics) and the distortion components (harmonics and interharmonics). Other rates, such as *THDG* and *THDS*, were normalised including interharmonics in the denominator, potentially leading to an underestimation of the total value. Furthermore, only some of the previous rates considered the stationarity of the signal. Therefore, in the literature, some authors have proposed new indices for evaluating harmonic disturbances in configurations related to power devices.

For example, the "*Short Time Disturbance Energy index for both the Low—and High-Frequency*" indices are defined in [34] and allow quantifying a large frequency spectrum (from 2 to 150 kHz). It provides a more accurate distortion evaluation using sliding windows of several sizes. However, in practical real-time measurements, these indices are very time-consuming, especially for non-stationary distortions; the equipment is also costly as collecting the high-frequency spectral components requires high sampling frequencies.
In [15-17], harmonics generated in the power grid by electric car chargers, photovoltaic inverters and further electronic devices are measured using factors of waveform distortion (*Fundamental Factor*, *FF*, and *Total Distortion Content*, *TDC*), and two new factors of waveform distortion are defined: *Total Harmonic-LF Factor* (THF_{LF}), and *Total Non-Harmonic-LF Distortion Factor* (*TNHDF*). These distortion factors allow measurement by differentiating only harmonics at low frequencies *(THF*), only interharmonics *(TNHDF*), and all harmonics and interharmonics *(TDC*). However, these factors normalise by the total rms value, thus including possible disturbances, and they also do not distinguish between high and low frequency harmonic distortion in their measurements.

In [18], the authors use the *THDS* subgroup distortion rate of the standard [14] to measure the distortion generated by grid-connected renewable energy converters. They also define two new distortion rates: *Total InterHarmonic Distortion Subgroup* ($TIHDS_{Y\,LF}$) for harmonic frequencies and *Total Harmonic and InterHarmonic Distortion Subgroup* ($TH\&IHDS_{Y\,HF}$) for supra-harmonic frequencies, which includes both harmonics and interharmonics and solves the problem of their evaluation at high frequencies. In [35], the *TIHDS* rate defined in [18] is improved by adding the interharmonic subgroups 0 and 1, thus allowing the evaluation of the first interharmonics between 10 and 90 Hz, which may contain helpful information about the status of the motors connected to the drives. The $TH\&IHDS_{Y\,HF}$ rate is again employed in [24] and [36], expanding the frequency range to 150 kHz. These rates solve the measurement problem by differentiating only the interharmonics and higher frequencies that are not considered in the standards. However, they still face two problems when measuring signals in drives: they normalise between the fundamental subgroup (with possible sidebands due to motor faults) and consider the fundamental frequency fixed, which is not the case in inverters.

It has been seen that none of the above rates describes the complete harmonic behaviour of inverters, so in the following section, a set of rates that fulfils that task will be proposed.

III. PROPOSED SET OF DISTORTION RATES FOR MEASURING DRIVE SIGNALS

Considering the qualities the rates for measuring drive signals already mentioned must meet and the limitations of the currently defined rates, a new set of rates is proposed, as shown in Table I. These rates are classified according to the frequency range addressed and the harmonic and interharmonic content measured, as shown in Fig. 1(a). They are also classified as dependent $TH\&IHD_{LF}$, $TIHD_{LFHF}$, $TH\&IHD_{LFHF}$ of the independent rates THD_{LF}, $TIHD_{LF}$, $TH\&IHD_{HF}$, as can be deduced from the expressions shown in Table I. The number of proposed rates is kept small for simplicity, given the large number of rates and distorting factors already existing in the literature.

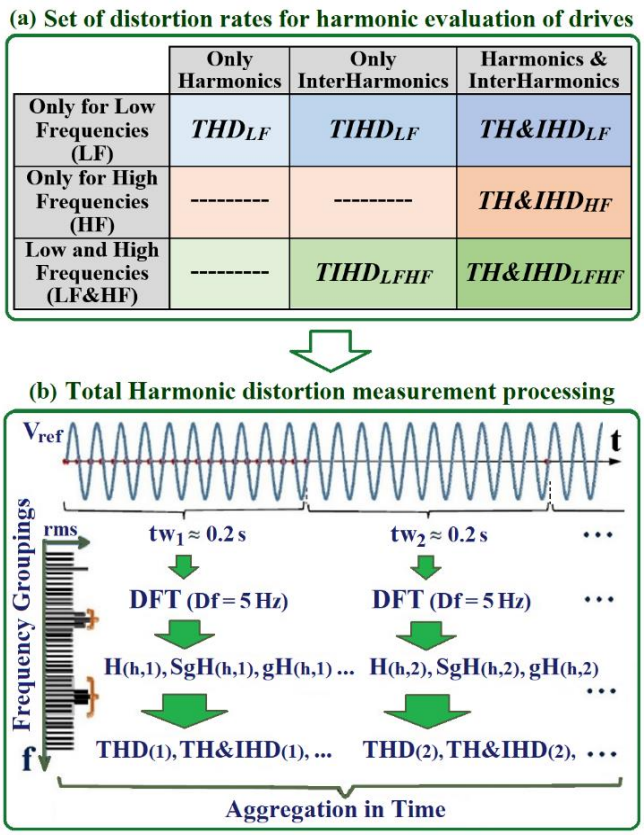

FIGURE 1. Summary of proposed distortion indices: (a) proposed rates classified by frequency range and harmonic and interharmonic content, (b) diagram of rates' processing in time and frequency domains.

The rates proposed in Table I stand out in three key aspects. They accommodate fundamental frequencies with a wide range of variation, offer variable LF and HF frequency ranges, and adapt the aggregation time to inverter signals (as will be seen in section IV). These proposed rates have some similarities with those of the standard [14] (THD_{LF}) and other

rates (also based on this standard) adapted by their authors for quality measurement in networks when power equipment is connected [18][24][35][36] ((*TIHD*$_{LF}$, *TH&IHD*$_{HF}$, similar to the rates of these authors, but normalising between the fundamental instead of the fundamental subgroup). The *TH&IHD*$_{LF}$ rate is akin to the *THDG* rate in the standard [14] but normalised only by the fundamental and including the first spectral bars contained in the interharmonic groups 0 and 1. The *TIHD*$_{LFHF}$ and *TH&IHD*$_{LFHF}$ rates are similar to the *TnHD* and *TWD* rates of [32,33] but processed following the standard [14], as will be discussed in Section IV and summarised in the diagram in Fig. 1(b).

As already indicated, among the qualities the proposed rates should meet, rate measurements with only harmonic content or only interharmonic content at high frequencies are not contemplated, so Fig. 1(a) shows these options empty. Furthermore, the limit used between low and high frequencies, *hmax*, is the 40 harmonic [14], but since there are different fundamental frequencies at the output of the drives, this limit is variable. For example, the top harmonic limit *hmax* would adopt values between 1600 and 2400 Hz for inverter output frequencies between 40 and 60 Hz.

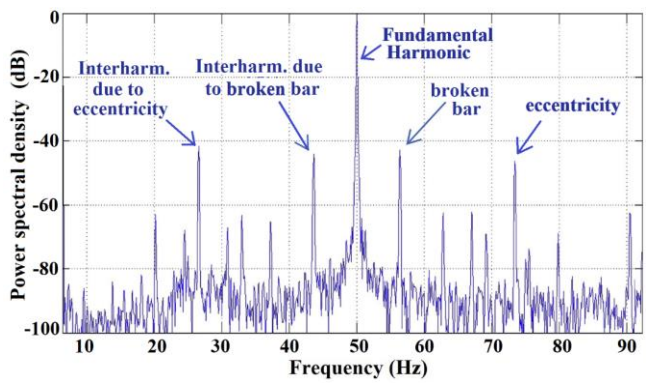

FIGURE 2. Spectra around main harmonic of an induction motor with a broken rotor bar and eccentricity [8].

All proposed rates in Table I are normalised by the fundamental. This allows for comparing measurements of drives connected to healthy motors, with little interharmonic content around the fundamental, with measurements of motors with some degree of failure that do present interharmonics close to the fundamental, as shown in Fig.2. So, it is convenient to avoid these frequencies close to the fundamental that can disturb this normalization. Normalising by the fundamental also does not consider the amplitude and phase modulation, typical of mains signals, which causes spectral sidebars around the fundamental. The fundamental is employed in the denominator to normalise the indices, where it is important that there are no interharmonics that could distort this normalisation. However, However, in the rate numerators, such as *TIHD*$_{LF}$, we have also considered the first two interharmonic groups, 0 and 1, similar to the rate proposed in [35]. Consequently, the measuring of interharmonics from 5 Hz to 95 Hz (for a 50 Hz grid) is included. Thanks to this, the *TIHD*$_{LF}$ rate can detect faulted motors because it considers interharmonics around the first harmonic that cause faults such as broken rotor bars, mixed eccentricity, and load unbalance [6,7], as will be seen at the end of Section V. However, the zero spectral bar or continuous component has not been considered since it incorporates the offsets of all measuring equipment and does not produce reliable data.

The equations in Table I use the nomenclature of the IEC 61000-4-7 standard [14] which will be presented in the next section, where the detailed explanation of the processing methods necessary to obtain these distortion rates will also be given.

IV. PROCESSING OF THE PROPOSED SET OF RATES

This section details how to process the proposed distortion rates, indicating the calculation procedure and the synchronism, frequency grouping and time aggregation methods used to reduce spectral leakage and its effects. It also explains how to evaluate the distortion for high frequencies.

A. RATE CALCULATION PROCEDURE

Techniques such as those based on Discrete Fourier Transform (DFT) are adequate for calculating the proposed rates since they do not need prior learning of the position and quantity of harmonic components of the analysed signals. Therefore, they can characterise harmonically any commercial inverter, given their great variety with multiple and unpredictable harmonic contents. DFT is a flexible, robust technique with a low computational burden and a good compromise between accuracy and simplification [37] compared to other parametric, nonparametric and hybrid harmonic analysis methods [32]. In order to unify measurements and make them comparable with other systems, the proposed rates will be processed based on methods defined by IEC 61000-4-30 and 61000-4-7 [13,14] for the measurement of harmonics and interharmonics, followed also by other international standards such as IEEE 519 [12].

The implementation of DFT in the analysis of frequency inverters is guided by the IEC standard, which recommends using rectangular windows of a constant length of 12/10 cycles for 60/50 Hz electrical networks, equivalent to about 0.2 s and a resolution of 5 Hz. The non-stationarity of the signals of the frequency inverters requires a balance between time and frequency resolution (uncertainty principle) [32,38]. This balance is maintained by choosing the sampling window during which the signals are analysed. The IEC standard indicates windows of 0.2 s for signals from the grid. However, this window duration must be adapted to the signal type analysed for other signals [39]. The windows used for the analysis of the inverter signals are as close as possible to the 0.2 s indicated in the standard, with a possible variation margin of 0.1 to 0.5 s, as specified in [40] for harmonics in industrial signals. This is done so that the

inverter signal measurements are comparable to those obtained with network signal standards, thus ensuring the accuracy of the proposed distortion rates.

DFT provides a reliable frequency analysis when the measured signal is stationary, so the signals analysed in the drives are only measured under stationary conditions. The sampling window is synchronised with the periods of every frequency component included in the analysed signal, particularly with the fundamental component and its harmonics. If the synchronism is lost or interharmonics are present, spectral leakage arises and causes unreliable measurements of the harmonic content of the evaluated signal.

For this reason, prior to using the DFT, spectral leakage generation is first reduced by synchronising the sampling window with the period of the current fundamental harmonic at the inverter output. Then, after the DFT is computed, the effects of spectral leakage are also diminished using the frequency and time groupings described in standards 61000-4-7 and 61000-4-30, as shown in the diagram in Fig. 1(b) and the flow chart in Fig. 3.

TABLE I
SET OF PROPOSED DISTORTION RATES FOR MEASUREMENT IN FREQUENCY CONVERTERS

Range	Name and definition of the rate:	Harmonics	Interharmonics	Related rates
LF (5 Hz-40○f1)	*Total Harmonic Distortion LF:* $THD_{YLF} = \sqrt{\sum_{h=2}^{hmax} \left(\frac{Y_{H,h}}{Y_{H,1}} \right)^2}$	✓	----	[14]
	Total InterHarmonic Distortion LF: $TIHD_{YLF} = \sqrt{\sum_{h=0}^{hmax} \left(\frac{Y_{ig,h}}{Y_{H,1}} \right)^2}$	----	✓	[18][24] [35][36]
	Total Harmonic & InterHarmonic Distortion LF: $TH\ \&\ IHD_{YLF} = \sqrt{\left(THD_{YLF} \right)^2 + \left(TIHD_{YLF} \right)^2}$	✓	✓	[14]
HF (41○f1-20 kHz)	*Total Harmonic & InterHarmonic Distortion HF:* $TH\ \&\ IHD_{YHF} = \frac{\sqrt{\sum_{h=hmax+1}^{20KHz} \left(Y_{sg,h} \right)^2 + \left(Y_{isg,h} \right)^2}}{Y_{H,1}}$	✓	✓	[18][24] [35][36]
LF & HF (5 Hz - 20 kHz)	*Total InterHarmonic Distortion LF&HF:* $TIHD_{YLFHF} = \sqrt{\left(TIHD_{YLF} \right)^2 + \left(TH\ \&\ IHD_{YHF} \right)^2}$	----	✓	[32][33]
	Total Harmonic&InterHarmonic Distortion LF&HF: $TH\ \&\ IHD_{YLFHF} = \sqrt{\left(THD_{YLF} \right)^2 + \left(TIHD_{YLF} \right)^2 + \left(TH\ \&\ IHD_{YHF} \right)^2}$	✓	✓	[32][33]

The symbol "Y" should be replaced by "V" for voltage and "I" for current. When nothing is indicated, it is understood that it refers to any of the signal types.

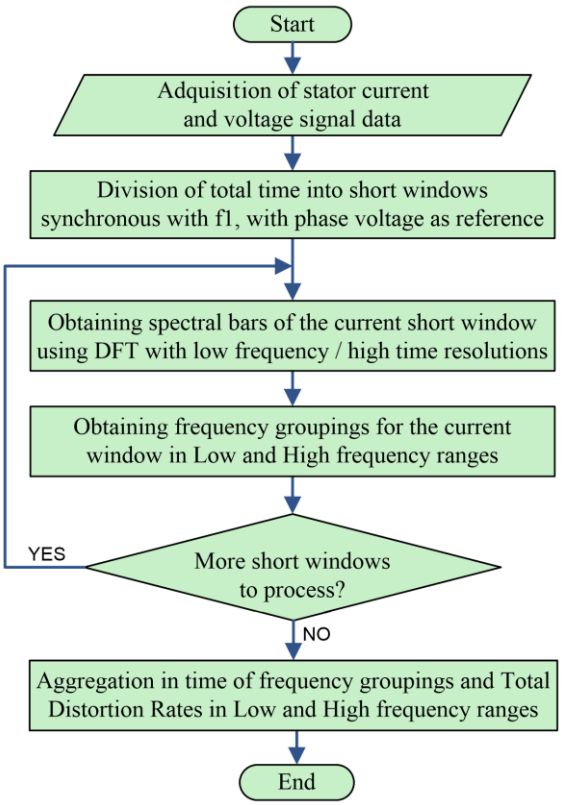

FIGURE 3. **Flowchart of the overall processing of total rates.**

To achieve synchronism, a previously filtered phase voltage is used as a reference signal to extract its fundamental harmonic, as shown at the top of the diagrams in Fig. 1(b) and Fig. 3. This is because it has been proven that the current signal increases the synchronism errors and thus the spectral leakage. In addition, because the output frequency of the drives changes to regulate the speed of the motors, synchronism must be achieved for a large range of fundamental frequencies. To adapt to this, the actual size of the sampling window is adjusted to the integer number of periods of the current frequency of the drive that most closely completes the standard short window (0.2 s).

Subsequently, with the frequency groupings of the spectral bars obtained after DFT, greater precision is achieved by absorbing a large part of the leakage generated inside the grouping and reducing the inaccuracy caused by the leakage radiated to the exterior. The frequency groupings indicated in the IEC 61000-4-7 standard are used [14], which are groups or subgroups of harmonics or interharmonics, to obtain the rates proposed in Table I. Harmonic groups ($Y_{g,h}$) weigh the rms value of every harmonic and all its neighbouring spectral bins. However, harmonic subgroups ($Y_{sg,h}$) evaluate the rms value of the harmonic and its two neighbouring bins. The harmonic subgroup helps measure the variations in the power grid's phase and amplitude of harmonics, which produce the bands adjacent to these harmonics. The interharmonic groups ($Y_{ig,h}$) and the interharmonic subgroups ($Y_{isg,h}$) evaluate the rms value of the spectral bins existing between adjacent harmonics without counting the bars contiguous to them for the interharmonic subgroups. Fig. 4 shows these groupings, using the frequency range between harmonics 4 and 9.

In addition to the previous considerations, the frequency groupings and resulting distortion rates must be aggregated in time to reduce the effects of spectral leakage and thus increase the accuracy of the measurements, as will be explained in the following subsection.

B. IMPROVEMENT OF RATE CALCULATION IN SIGNALS WITH HIGH INTERHARMONIC INTERACTION

Harmonic measurements based on IEC standards present a problem due to the instability and imprecision of the rms values obtained in consecutive analysis windows when performing DFT. This is a direct result of the spectral leakage produced by one or several interharmonic tones close to each other. The reason is that the spectral leakage modifies the phases of the tested interharmonics and the magnitudes of the vectors obtained by summing the total of the components in every spectral bin [41]. These fluctuations affect both frequency groupings and distortion rates. It will be shown that this problem is overcome by aggregating in time to minimise the influence of leakage on the amplitude fluctuation obtained and thus achieve a more stabilised and accurate rms result.

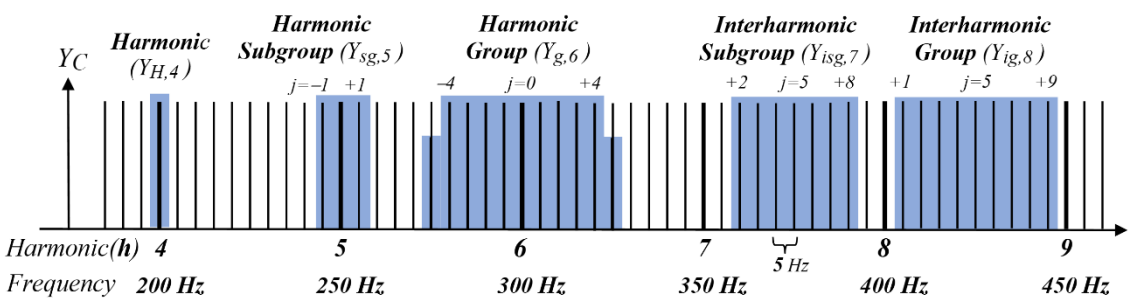

FIGURE 4. **Representation of the harmonic of order 4, $Y_{H,4}$, harmonic subgroup of order 5, $Y_{sg,5}$, harmonic group of order 6, $Y_{g,6}$, interharmonic subgroup of order 7, $Y_{isg,7}$, and interharmonic group of order 8, $Y_{ig,8}$, for a fundamental of f_1 =50 Hz.**

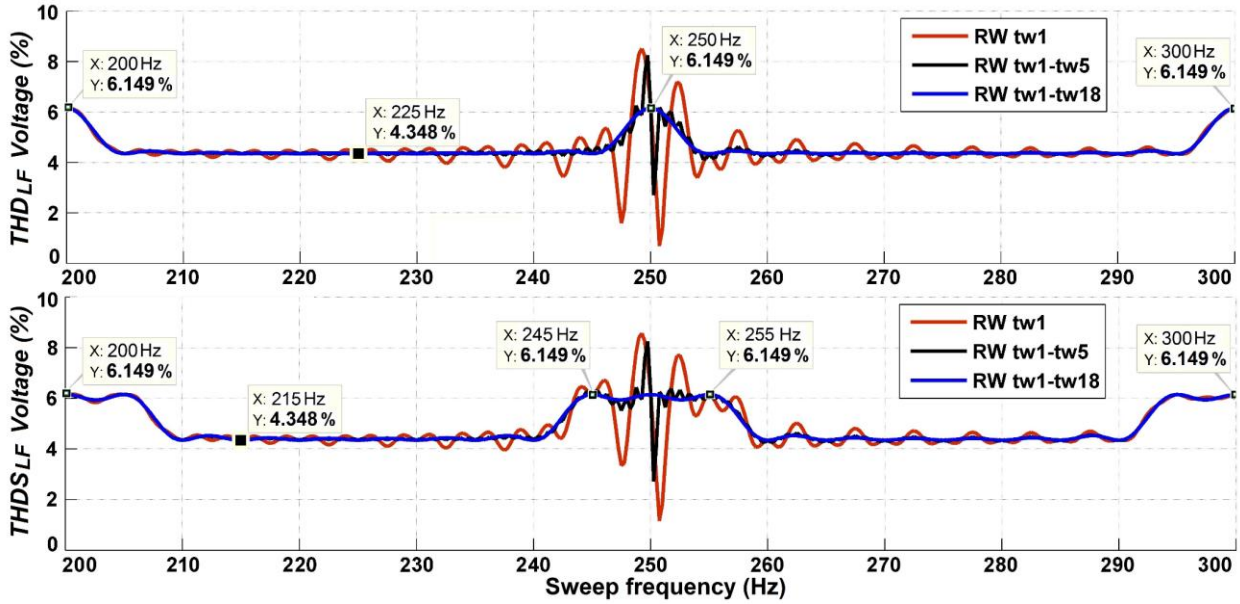

FIGURE 5. **Distortion rates for sweep tone and 5th harmonic without aggregation, red line, and with time aggregation (aggregating the initial 5 windows, black line, and with many windows added, blue line).**

Fig. 5 shows the low frequency THD_{LF} and $THDS_{LF}$ rates found for a signal with a 5th harmonic of 10 Vrms at 250 Hz and an interharmonic tone of the same amplitude 10 V with variable frequency assigned to the horizontal axis, whose spectral leakage interacts with the fixed harmonic. The distortion rates are normalised assuming a 230 V fundamental and found for successive rectangular windows: without aggregation, red line, and with time aggregation (aggregating the initial 5 windows, black line, and with many windows added, blue line).

When dealing with a single tone or distant tones that do not interact, the values of the rates found by DFT remain consistent during consecutive windows analysed. This is evident in Fig. 5 when the sweep tone is distant from the harmonic at 250 Hz. However, when tones with close interharmonics interact, the values produced in consecutive windows show a noticeable fluctuation. The most significant variations occur when the interacting tones are in close proximity, as illustrated by the position of the sweep tone near 250 Hz, where the harmonic is located.

For synchronous sweep tone frequencies (multiples of the 5 Hz resolution), the measured value has no error as no spectral leakage is generated since the periods are exact multiples of the 0.2 s window applied. On the other hand, interharmonic or non-synchronous frequencies generate spectral leakage that radiates from the considered harmonic grouping outward when the tone is inside and inward when the variable tone is outside. The most significant leakage is generated when the variable tone is located in intermediate positions between consecutive spectral bars. In these cases, the rms values produced are most different from the correct ones.

Observing Fig. 5, in the positions where the sweep tone presents harmonic values (multiples of 50 Hz), or its sidebands at ± 5 Hz for the case of the *THDS* subgroup rate, the value obtained is $\sqrt{10V^2 + 10V^2}/_{230\ V}$ = 6.149 %, since the fixed harmonic always at 250 Hz is added to the variable tone that is also adopting in those cases a harmonic position. On the other hand, in other positions of the sweep tone, the value of the rates should be $\sqrt{10V^2}/_{230\ V}$ = 4.348 % although, due to spectral leakage, this only occurs accurately in the synchronous positions or multiples of 5 Hz, in which the sweep tone does not emit leakage.

All of the above can be generalized for any quantity of interharmonic tones, with the largest amplitude fluctuations when performing DFT in consecutive sampling windows in the spectral bins close to interacting tones and leak generators, in contrast to minor variations in those farther away.

The way to mitigate these amplitude variations due to spectral leakage is by aggregating over time the RMS values found in the successive windows analysed, using the square root of the arithmetic mean of the squared RMS values. This time aggregation should be applied to all frequency groupings and distortion indices (as these groupings form them), as seen at the bottom of the diagrams in Fig. 1(b) and Fig. 3. As illustrated in Fig. 5, this process enhances the stability and reliability of the values obtained, contrasting the results with and without aggregation (blue versus red) or with insufficient aggregated windows (blue versus black).

IEC standard time groupings are convenient for harmonic analysis of real electrical network signals at 3 s, 10 min and 2 h periods [13]. However, this time aggregation must be adapted to the thermal time coefficients of the attached devices: the 3 s aggregation interval is recommended for industrial environments characterised by short thermal time

constants; other intervals are more suitable for systems with longer constants [32,38]. Then, the aggregation time must be adapted to analyse the output signals of frequency converters, with harmonic content different from that of the power grid, since this time will also depend on the characteristics of the test, class of frequency converter and supported load [42].

Fig. 6 shows the evolution of some distortion indexes for the output voltage of an Altivar 66 inverter using 0.2 s rectangular windows. The plots in red are for rates without time aggregation, and the plots in blue are for rates with aggregation times from 0.2 seconds to 60 seconds. The points corresponding to 10 seconds of time aggregation and 50 0.2-second windows are labelled. The analysis reveals that the rates and groupings exhibit less variation when covering more frequencies. The rms presents the lowest percentage of changes, followed by the $TH\&IHD_{LFHF}$ and $TH\&IHD_{HF}$ rates, which also gauge extensive harmonic contents. These rates vary little and are not significantly influenced by the total aggregation time. This could be attributed to the compensatory effect of adding the spectral leakage of numerous components, thereby minimizing errors due to leakage. Conversely, rates and groups with lower harmonic content, due to leakage interactions between close interharmonics, exhibit more fluctuations and therefore require longer aggregation time, as evidenced in Fig. 6 with rates such as $TIHD_{LF}$ and THD_{LF} and especially in simple groups such as $SgIH_5$.

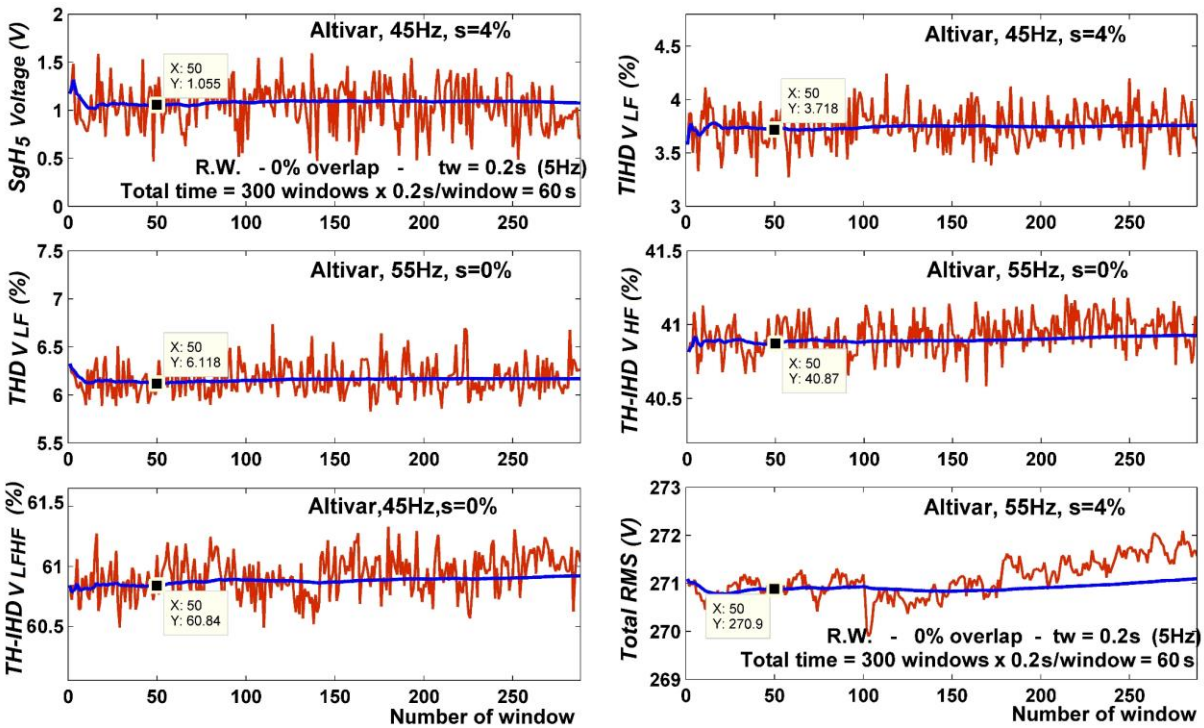

FIGURE 6. Evolution over time of the $SgIH_5$ subgroup and rates $TIHD_{LF}$, THD_{LF}, $TH\&IHD_{HF}$, $TH\&IHD_{LFHF}$, and total RMS (in red without aggregation, and in blue with time aggregation).

Therefore, the appropriate aggregation time depends on the conditions of every test and even on the type of measurement (harmonic groups or distortion rates). The output signals of drives with high interharmonic content need a higher aggregation time to stabilize the results. Fig. 6 illustrates that an aggregation time of 3 s is not always enough to stabilize the result, prompting an extension of this value. However, reaching the next value of 10 min indicated in the standards would be excessive. Tests with low-power drives have shown that an aggregation time of about 10 s provides much more stable measurements than those with 3 s. Consequently, 10 s has been chosen as the common aggregation time for all measurements in the tested drives.

C. MEASUREMENTS ABOVE HARMONIC FREQUENCIES

The IEC 61000-4-7 standard [14], among the standards for measurement in the supra-harmonic frequency band, defines a technique for assessing harmonic distortion up to 9 kHz, recently extended to 150 kHz for illustrative applications. Measurement in this high-frequency range does not require high-frequency resolution, and no distinction is made between harmonics and interharmonics. DFT is used for the frequency domain analysis with rectangular windows of approximately 0.2 s (5 Hz resolution). The IEC 61000-4-30 standard [13] proposes an experimental technique for measurements in the frequency band between 2 and 150 kHz, where a small analysis window of 0.5 ms (2 kHz resolution) is used. A high

sampling frequency is needed, and the data would be extensive if the window were longer, although the IEC 61000-4-7 method is still considered valid. A comparison between these techniques ([14] and [13]) is presented in [43,44], showing that the IEC 61000-4-7 method has a higher signal-to-noise ratio and is more robust and accurate than the IEC 61000-4-30 method.

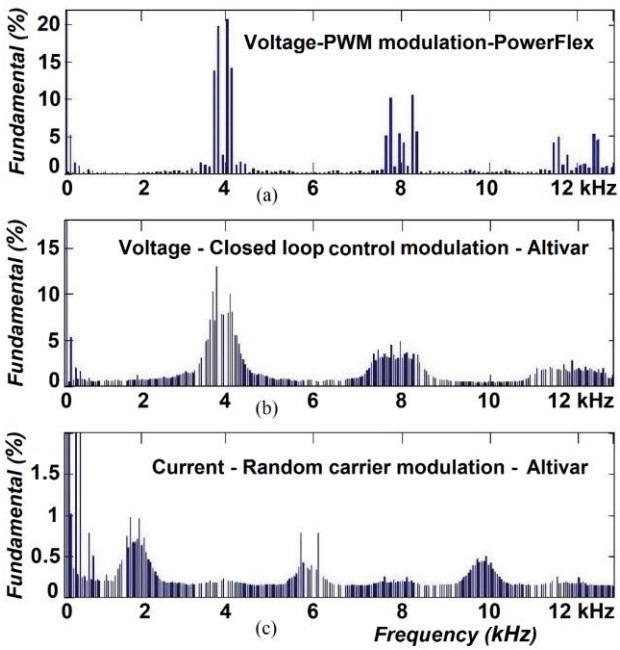

FIGURE 7. Spectra of inverters tested in section V with different types of modulation: (a) PowerFlex (PWM), (b) Altivar (modulation with closed-loop control) and (c) Altivar (random carrier PWM modulation).

On the other hand, it can be helpful to find distortion indices containing frequency groupings in particular high-frequency zones with high interharmonic density, where the location of supraharmonics is associated with the commutation frequency and its multiples, as occurs with inverter outputs using PWM modulations [45-47]. Inverters that use other modulation types, such as modulation with closed-loop control and Random Carrier PWM type, have a more dispersed harmonic content at high frequencies and are not necessarily concentrated around multiples of switching frequencies (see Fig. 7).

Therefore, high frequencies are measured based on IEC 61000-4-7 [14] in this proposed methodology, and all the spectral bars contained in the complete high-frequency range are also considered, not only those located around multiples of the switching frequencies. This way, the resulting $TH\&IHD_{HF}$ rate can be used to measure the high-frequency harmonic content globally and independently of the type of modulation used by each drive.

V. EXPERIMENTAL RESULTS AND DISCUSSION

The proposed methodology has been experimentally verified using low power frequency converters, consisting of a rectifier and a voltage source inverter, with different modulation types and harmonic content (with spectra as different as those shown in Fig. 7). They have been tested feeding induction motors with different operating states and working with low and high loads (slip "s" between 0.3 and 4%). Two Siemens motors were used with the specifications indicated in Table II. One of them was healthy, and the other suffered from mixed eccentricity. Inverters with the specifications listed in Table II were tested and configured to operate with the following control modes:

- PowerFlex-40 drive, with PWM modulation and Scalar mode control (SCAL).
- PowerFlex-40 inverter, with PWM modulation and Vector mode control (VECT).
- Altivar-66 drive, with closed loop PWM modulation and Constant Torque control, in Normal mode (CTN) or Special mode (CTS).
- Altivar-66 inverter, with random carrier PWM modulation for low acoustic noise and Variable Torque control, in Normal (VTN) or non-Load (VTnL) mode.
- Power supply from the Mains.

The drives' phase voltage and output current signals were sampled and digitized with a National Instruments PCI6250 acquisition card, following a stage of electrical isolation and conditioning based on Hall effect probes by LEM. The MATLAB software package was then used to control the signal acquisition and post-process the stored data. All measurements were performed at the output of the inverters, in steady state during 60 s tests, and with a sampling frequency of 80 kS/s. This high sampling frequency was chosen to meet all the necessary specifications, ensuring accurate measurement of the high harmonics of the inverters, reducing noise, and minimizing synchronism errors due to the sampling interval. Fig. 8 shows the laboratory test bench used for the experiments, and Fig. 9 shows the schematic diagram for the proposed drive system.

Next, some measurement examples are shown. The first examples allow for the observation of the relationships between the dependent and independent rates for each spectrum zone, according to the harmonic and interharmonic content. The following examples will compare the harmonic behaviour between different drives, observing the dependence of the rates with the variable parameters used in the tests, such as the drive control and modulation type, the fundamental output frequency, the switching frequency, the load level, and the type of motor, healthy or faulty.

Fig. 10 shows these three low-frequency rates: the distortion rate for harmonics only, the interharmonics-only rate, and the total rate for harmonics and interharmonics. These rates are shown for different values of the output frequency of the PowerFlex 40 inverter functioning in vector mode and feeding an induction motor at rated load. The analysis of Fig. 10(a), which displays the rates for the current signal, shows an equal distribution between harmonics (THD_{ILF}) and interharmonics ($TIHD_{ILF}$), with a higher interharmonic content up to the nominal frequency (50 Hz). In contrast, the voltage rates (Fig.

10(b)) exhibit a higher harmonic content: THD_{VLF} is considerably higher than $TIHD_{VLF}$. So, the total rates at low frequencies $TH\&IHD_{LF}$ more closely resemble the majority components in each case. An increase in $TH\&IHD_{ILF}$ rate is observed as the fundamental output frequency increases, especially from the nominal frequency, due to the overmodulation in the inverter coming into operation from that frequency onwards.

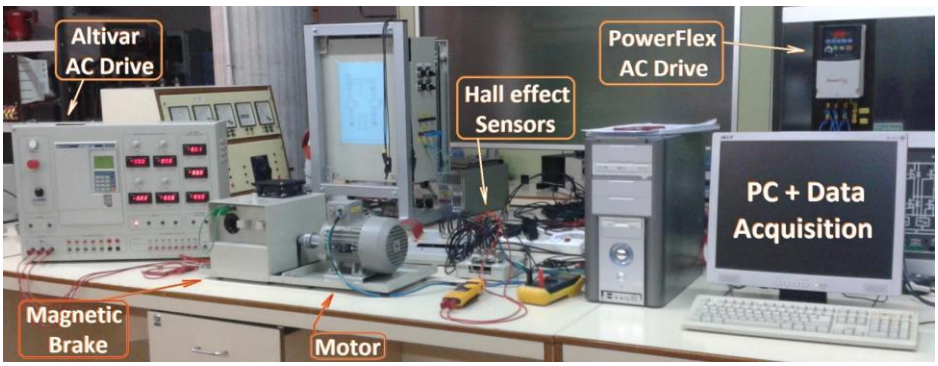

FIGURE 8. **Laboratory test bench used in the experiments.**

In Fig. 11, the graph displays the total harmonic and interharmonic rates for low frequencies, high frequencies, and the combination of both. These rates are based on the same drive and load, as shown in Fig. 10. Fig. 11(a) indicates a similar distribution between the total high and low frequency current signal rates, with slightly higher $TH\&IHD_{IHF}$ than $TH\&IHD_{ILF}$ up to the nominal frequency. On the other hand, Fig. 11(b) shows that the high-frequency harmonic content measured by the $TH\&IHD_{VHF}$ voltage rate is much higher than the corresponding low-frequency $TH\&IHD_{VLF}$, resulting in the total $TH\&IHD_{VLFHF}$ voltage rate being primarily composed of the $TH\&IHD_{VHF}$ rate. Additionally, it is observed that the latter voltage rate decreases as the fundamental output frequency increases, stabilizing from the nominal frequency. Regarding the current, the total rate of $TH\&IHD_{ILFHF}$ increases with the fundamental, mainly due to the contribution of low frequencies $TH\&IHD_{ILF}$.

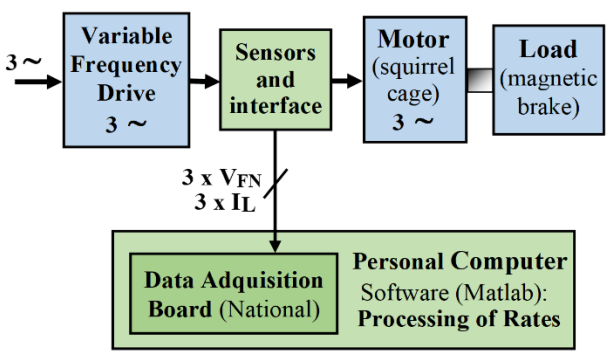

FIGURE 9. **Block diagram of the test bench, with the proposed drive system (blue) and the measurement and analysis equipment (green).**

Fig. 12 shows rates corresponding only to interharmonics at low frequencies, at high frequencies and the combination of the two. These indices have been computed on the stator current signal for the same drive as Fig. 10 and 11. Load variation impacted the low-frequency interharmonics rate, $TIHD_{ILF}$. It is higher for high loads (Fig. 12(a), with slip s = 4%) and decreases slightly for high-frequency interharmonics, $TH\&IHD_{IHF}$, with respect to low loads (Fig. 12(b)). As the low-frequency interharmonic rate is lower than the high-frequency rate for the stator current signal, the rate that combines both, $TH\&IHD_{ILFHF}$, more closely resembles the latter.

TABLE II
RATINGS OF THE COMPONENTS USED IN EXPERIMENTAL SETUP

INVERTERS	PowerFlex 40 22B-D6P0N104	Altivar 66 ATV-66U41N4
Rated power	2.2 kW	2.2 kW
Input voltage range	342 V – 528 V	340 V – 530 V
Output voltage	0 – 460 V	0 – 460 V
Rated input current	7.5 A	8 A
Max. output current	6 A	5.8 A
Input frequency	48 – 63 Hz	47.5 – 63 Hz
Output frequency	0 – 400 Hz	0.1 – 400 Hz
MOTOR	Siemens 1LA7083–4AA10	
Frequency	50 Hz	60 Hz
Rated power	0.75 kW	0.86 kW
Rated voltage	230/400 V Δ/Y	460 V Y
Rated current	3.2/1.86 A Δ/Y	1.8 A Y
Rated speed	1395 1/min	1695 1/min
Cos (φ)	0.81	0.81

Fig. 13(a) reveals that the switching frequency of the PowerFlex drive has little influence on the $TH\&IHD_{VHF}$ high-frequency voltage distortion rate, although this rate decreases with the fundamental output frequency. In contrast, the current high-frequency rate $TH\&IHD_{IHF}$ is hardly affected by the fundamental output frequency of the drive, but increasing the switching frequency reduces the current high-frequency

harmonic and interharmonic contents, as seen in Fig. 13(b). It has been verified in all tests that this was the only case where the switching frequency influenced the rate variation, only for high-frequencies of the current signal.

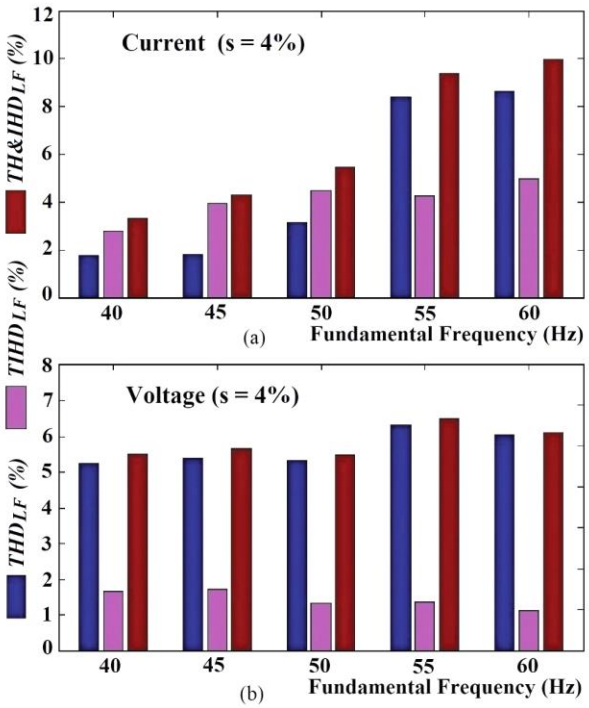

FIGURE 10. Relationships between low frequency rates for harmonics THD_{LF}, interharmonics $TIHD_{LF}$, and total for harmonics and interharmonics $TH\&IHD_{LF}$, as a function of fundamental frequency, for (a) current, and (b) voltage.

In conclusion, it will be demonstrated that the comprehensive set of rates developed allows for comparing the harmonic behaviour of different drives and, consequently, their performance in powering motors prone to fault diagnosis. This is made possible by observing the distortion rates developed, which are based on standards, unifying the approach to all measurements.

The total low-frequency rates, $TH\&IHD_{ILF}$ and $TH\&IHD_{VLF}$, tend to increase with the fundamental output frequency, especially for the current signal (Fig. 14(a)). These increases are justified by the growth of the harmonic part (THD_{ILF}) for the current signal, and the growth of the interharmonic part for the voltage signal ($TIHD_{VLF}$) in the Altivar inverter case, as shown in Fig. 15. Therefore, the harmonic contamination in these inverters is avoided, in the low-frequency range, below the 50 Hz output frequency. This pollution is produced by overmodulation from this nominal frequency, especially for the noisiest drives at low frequencies, such as the Altivar drive working in its VTx modes (for voltage) and the PowerFlex drive in its scalar and vector modes (for current).

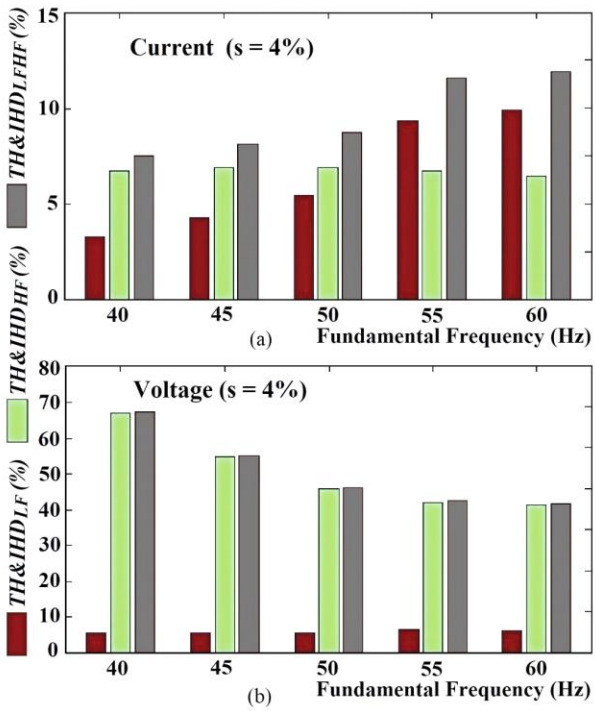

FIGURE 11. Relationships between total rates for low frequency $TH\&IHD_{LF}$, high frequency $TH\&IHD_{HF}$, and for low and high frequency $TH\&IHD_{LFHF}$, as a function of fundamental, for (a) current, and (b) voltage.

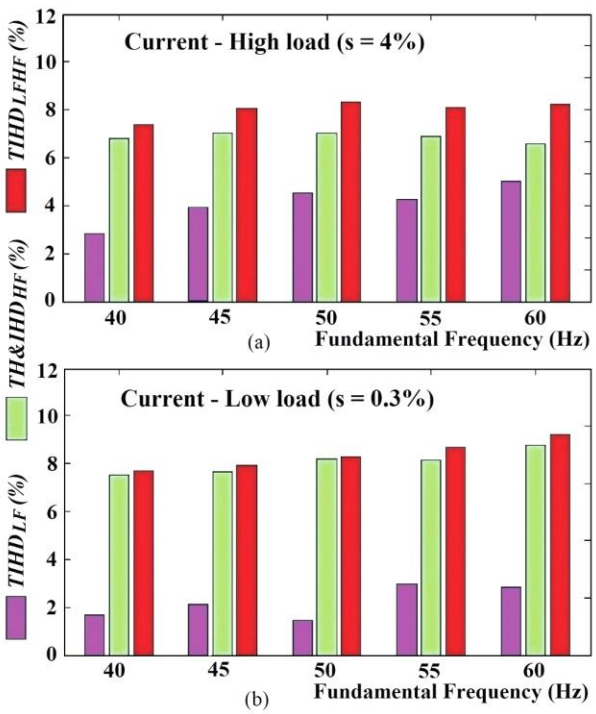

FIGURE 12. Relationships between the current signal interharmonic-only rates for low frequency $TIHD_{ILF}$, high frequency $TH\&IHD_{IHF}$, and for low and high frequency $TIHD_{ILFHF}$, as a function of fundamental, for (a) nominal load, and (b) low load.

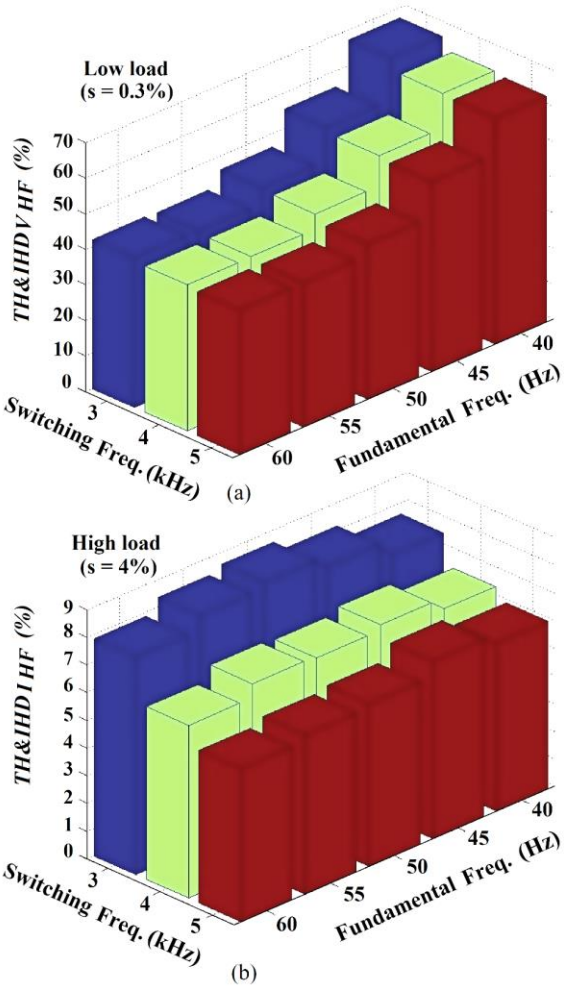

FIGURE 13. **Distortion rates as a function of fundamental output and switching frequencies, in PowerFlex drive in scalar mode, for: (a) voltage high frequency *TH&IHD$_{VHF}$* and low load, (b) current signal high frequency *TH&IHD$_{IHF}$* and high load.**

The total high-frequency rates follow the opposite trend from that seen for low frequencies since the harmonic content at high frequencies decreases with the fundamental output frequency, especially the voltage rate (Fig. 16(b)). In addition, the harmonic content at high frequencies is much higher for the voltage signal due to the motor's filtering effect on the current, which is practically non-existent in the case of mains supply. Therefore, to work with the least harmonic pollution in the high-frequency region it is better to operate above the rated frequency, especially for the noisiest high-frequency drive, which in this case is again the Altivar in its VTx modes (both voltage and current) due to its random carrier modulation system.

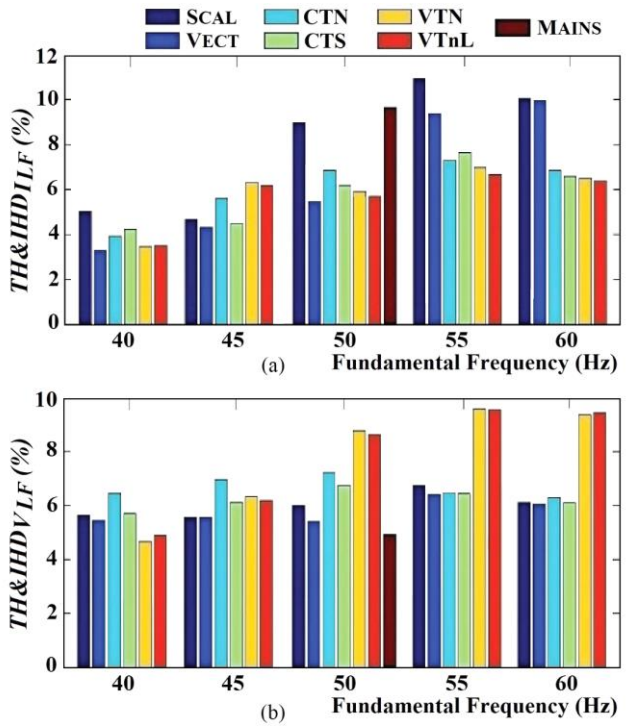

FIGURE 14. **Evolution with output frequency of total distortion rates for low frequency of (a) current *TH&IHD$_{ILF}$*, and (b) voltage *TH&IHD$_{VLF}$*, for the different control modes and drives tested.**

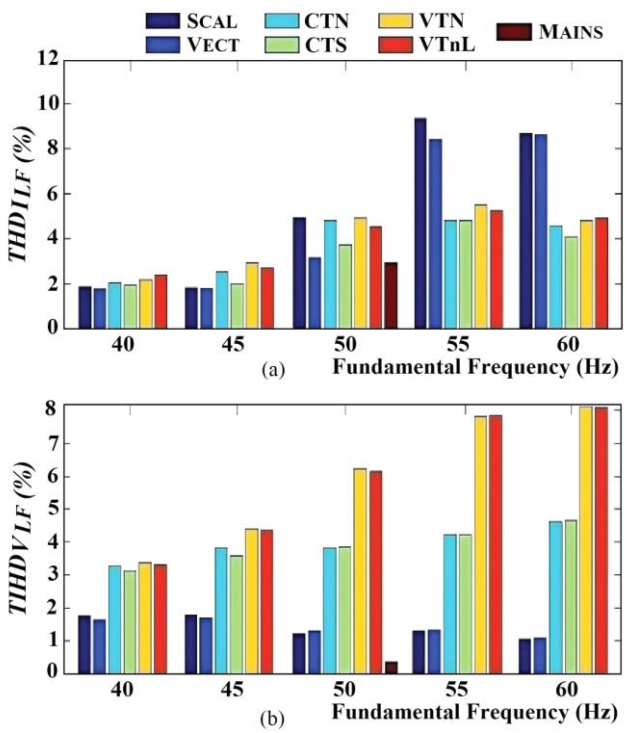

FIGURE 15. **Evolution with output frequency of the partial distortion rates for low frequency of (a) harmonics of current *THDI$_{LF}$* , and (b) voltage interharmonics *TIHDV$_{LF}$*, for the control modes and drives tested.**

Thus, the lowest harmonic distortion at low frequencies has been below the nominal output frequency. In addition, the noisiest drives have been those using PWM modulation for current and random carrier modulation for voltage at low frequencies. On the other hand, at high frequencies, the lowest harmonic contents have been above the nominal frequency, especially with PWM modulations that produce fewer interharmonics at high frequencies than random carrier or closed-loop control modulations. Moreover, this high-frequency distortion decreases by increasing the switching frequency and load.

These rates can be used to assess faulty motors, such as those with mixed eccentricity. The analysis revealed significant differences in the low-frequency region between healthy and defective motors at high loads and for fundamental output frequencies lower or equal to the nominal frequency. The $TIHD_{ILF}$ rate, which considers interharmonics in the current signals, identifies motors with high severity mixed eccentricity. Fig. 17 illustrates the percentage differences between the $TIHD_{ILF}$ rates of a healthy motor and one with mixed eccentricity. The negative values indicate that the rate of the motor with eccentricity is higher, as shown in the upper part (a) of the figure for the high load case.

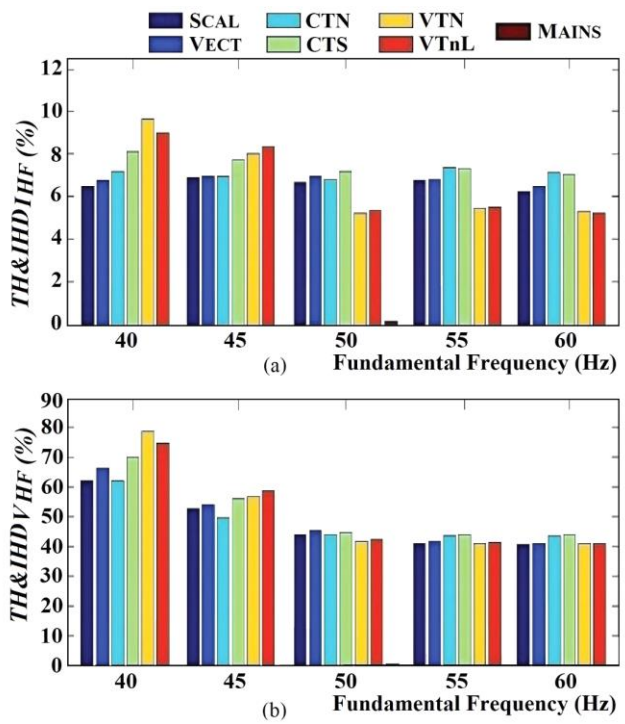

FIGURE 16. Evolution with output frequency of total distortion rates for high frequency of (a) current $TH\&IHD_{IHF}$, and (b) voltage $TH\&IHD_{VHF}$, for the different control modes and drives tested.

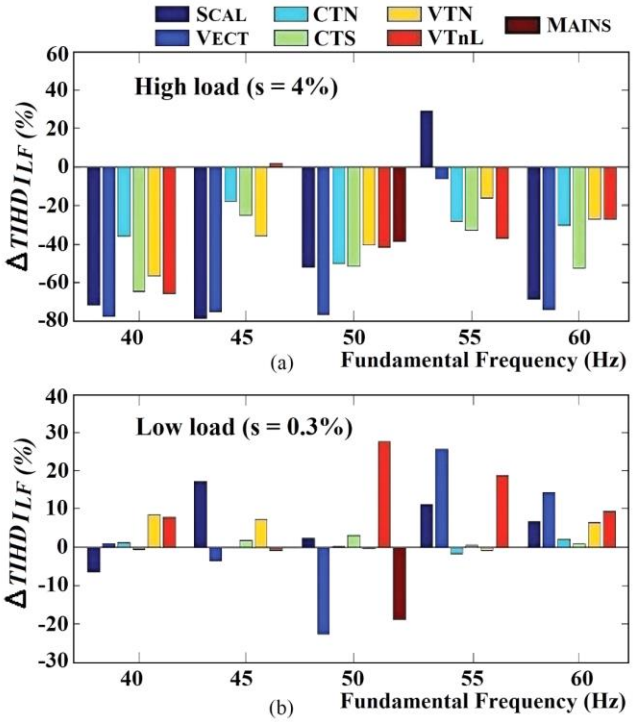

FIGURE 17. Evolution with output frequency of the relative differences between the current interharmonic distortion rates $TIHD_{ILF}$ of a healthy motor and a motor with eccentricity, (a) at nominal load, and (b) at low load, for the control modes and drives tested.

VI. CONCLUSIONS

Variable-frequency drives generate harmonics that may harm the induction motors they supply and make fault detection difficult. Therefore, it is advisable to measure their harmonic content to determine the quality of the power supplied and thus facilitate the prevention and diagnosis of possible anomalies. Consequently, this work proposes a methodology to characterize their output harmonic content based on a set of distortion rates specially processed to adapt them to the special features of the inverters' output signals.

Then, a set of rates has been proposed for the distortion characterisation of inverters' output. These rates are based on the IEC standards due to their satisfactory compromise between accuracy, simplification, and unification of measurements with those of commercial power quality meters that follow these same standards. However, it has been necessary to adapt these rates to the unique characteristics of the inverter output signals. These new rates have to synchronise with different fundamental frequencies, allow for the measurement of harmonics and interharmonics, differentiate each type of component in low- and high-frequency areas, cover a broader range of frequencies, and be adequately normalised. These rates complement and improve those established in the standards and literature and adapt better to measuring distortion in inverters' signals.

In addition to the above, the following conclusions have been reached in this article:

- The distortion rates vary significantly when the DFT is performed over successive time windows due to the interaction of spectral leakage generated between nearby interharmonics, such as those produced at the output of the drives, producing inaccurate results. This problem is minimised by aggregating in time the successive rates obtained.
- The analysis of the influence of the aggregation time has made it possible to foresee the need for a longer aggregation time for signals with abundant interharmonic components, such as those appearing at the output of inverters. It has also been found that rates evaluating wider frequency ranges and with higher harmonic content require shorter aggregation times than those covering smaller spectrum areas.
- As part of the proposed methodology, a comprehensive test plan has been developed. This plan is designed to deduce the optimum conditions for the minimum harmonic emission of the drives. Once identified, these optimum conditions can be practically applied to reduce losses in the motor and improve its diagnostics.
- It has been seen that the power supplies with the highest distortion rates at low frequencies are those using PWM modulation for current, random carrier modulation for voltage, and output frequencies higher than nominal. At high frequencies, on the other hand, the power supplies with the highest distortion rates are the ones with frequencies lower than nominal, low switching frequencies, low load, and always of the random carrier modulation type.
- Rates considering interharmonics at the low range of the current spectrum successfully detected faults in motors with mixed eccentricity highly loaded and fundamental output frequencies lower or equal to the rated one. These are the optimal conditions for the detection.

In summary, this work has proposed a methodology that allows for the characterisation of the harmonic behaviour of different low power frequency inverters in actual operating conditions. This methodology unifies how measurements are performed, using a set of new distortion rates processed by adjusting them to the characteristics of the output signals of the electronic converters. The proposed method enables the comparison of the drives' performance and contributes to the field by reducing motor losses and improving the prevention and diagnosis of failures. Future research could extend the range of tests to higher power motors and drives, with spectra different from those tested in this article, demonstrating the validity of the proposed method to characterise any inverter.

REFERENCES

[1] A. Gudiño-Ochoa, J. Jalomo-Cuevas, J. E. Molinar-Solís, and R. Ochoa-Ornelas, "Analysis of Interharmonics Generation in Induction Motors Driven by Variable Frequency Drives and AC Choppers," Energies, vol. 16, no. 14, 2023.

[2] V. Fernandez-Cavero, L. A. Garcia-Escudero, J. Pons-Llinares, M. A. Fernandez-Temprano, O. Duque-Perez, and D. Morinigo-Sotelo, "Diagnosis of broken rotor bars during the startup of inverter-fed induction motors using the dragon transform and functional anova," Appl. Sci., vol. 11, no. 9, 2021.

[3] C. Huang, S. Bu, H. H. Lee, K. W. Chan, and W. K. C. Yung, "Prognostics and health management for induction machines: a comprehensive review," J. Intell. Manuf. vol. 35, no. 3, pp. 937-962, 2024.

[4] T. Garcia-Calva, D. Morinigo-Sotelo, V. Fernandez-Cavero, and R. Romero-Troncoso, "Early Detection of Faults in Induction Motors-A Review," Energies, vol. 15, no. 21, pp. 1-18, 2022.

[5] W. T. Thomson and I. Culbert, Current Signature Analysis for Condition Monitoring of Cage Induction Motors: Industrial Application and Case Histories. Hoboken, NJ, USA: Wiley, 2017.

[6] G. Niu, X. Dong, and Y. Chen, "Motor Fault Diagnostics Based on Current Signatures: A Review," IEEE Trans. Instrum. Meas. vol. 72, pp. 1-19, 2023.

[7] M. F. Yakhni et al., "Variable speed induction motors' fault detection based on transient motor current signatures analysis: A review," Mech. Syst. Signal Process. vol. 184, no. September 2022, p. 109737, 2023.

[8] O. Duque-Perez, L. A. Garcia-Escudero, D. Morinigo-Sotelo, P. E. Gardel, and M. Perez-Alonso, "Analysis of fault signatures for the diagnosis of induction motors fed by voltage source inverters using ANOVA and additive models," Electr. Power Syst. Res. vol. 121, pp. 1-13, 2015.

[9] L. Alhafadhi and J. Teh, "Advances in reduction of total harmonic distortion in solar photovoltaic systems: A literature review," Int. J. Energy Res., vol. 44, no. 4, pp. 2455-2470, 2020.

[10] L. J. Varghese, R. Gandhi Raj, R. S. Ravi Sankar, and Z. Tan, "Design of Total Harmonic Distortion Reduction using Quantum Coyote Optimization Algorithm for Hybrid Power Generation Systems," Journal of Circuits, Systems and Computers, vol. 32, no. 17, p. 2350287, 2023.

[11] R. Martinek, J. Rzidky, R. Jaros, P. Bilik, and M. Ladrova, "Least mean squares and recursive least squares algorithms for total harmonic distortion reduction using shunt active power filter control," Energies, vol. 12, no. 8, p. 1545, 2019.

[12] IEEE Standard 519-2014, Ed., IEEE 519 Recommended Practice and Requirements for Harmonic Control in Electric Power Systems. New York, NY, USA: IEEE, 2014.

[13] International Electrotechnical Commission (IEC), Ed., IEC Standard 61000-4-30: Testing and Measurement Techniques-Power Quality Measurement Methods. Geneva, Switzerland: IEC, 2015.

[14] International Electrotechnical Commission (IEC), Ed., IEC Standard 61000-4-7: General Guide on Harmonics and Interharmonics Measurements, for Power Supply Systems and Equipment Connected Thereto. Geneva, Switzerland: IEC, 2010.

[15] X. Xu, "Harmonic Modelling and Characterisation of Modern Power Electronic Devices in Low Voltage Networks," Ph.D. Thesis, The University of Edinburgh, Edinburgh, UK, 2018.

[16] X. Xu et al., "On the impact of operating modes and power supply conditions on the efficiency of power electronic devices," 2016 IEEE Int. Work. Appl. Meas. Power Syst., pp. 1-6, 2016.

[17] X. Xiao et al., "Analysis and Modelling of Power-Dependent Harmonic Characteristics of Modern PE Devices in LV Networks," IEEE Trans. Power Deliv. vol. 32, no. 2, pp. 1014-1023, 2017.

[18] R. Langella, A. Testa, J. Meyer, F. Moller, R. Stiegler, and S. Z. Djokic, "Experimental-Based Evaluation of PV Inverter Harmonic and Interharmonic Distortion Due to Different Operating Conditions," IEEE Trans. Instrum. Meas. vol. 65, no. 10, pp. 2221-2233, 2016.

[19] R. Mohanty et al., "Lower Output Voltage Harmonics With Optimum Switching Angles of Single PV-Source Based Reduced Switch Multilevel Inverter Using BWO Algorithm," IEEE Access, vol. 12, pp. 5054-5065, 2024.

[20] A. Mishra and K. Chatterjee, "Harmonic analysis and attenuation using LCL-filter in doubly fed induction generator based wind conversion system using real time simulation based OPAL-RT," Alexandria Eng. J., vol. 61, no. 5, pp. 3773-3792, 2022.

[21] B. Selma, E. Bounadja, B. Belmadani, B. Selma, and M. Fliess, "A novel intelligent control approach for wind energy conversion systems

with synchronous reluctance generators," Int. J. Circuit Theory Appl., no. January, pp. 1-21, 2024.
[22] A. Kazemtarghi, A. Chandwani, N. Ishraq, and A. Mallik, "Active Compensation-Based Harmonic Reduction Technique to Mitigate Power Quality Impacts of EV Charging Systems," IEEE Trans. Transp. Electrif. vol. 9, no. 1, pp. 1629-1640, 2023.
[23] A. Srivastava, M. Manas, and R. K. Dubey, "Electric vehicle integration's impacts on power quality in distribution network and associated mitigation measures: a review," J. Eng. Appl. Sci., vol. 70, no. 1, pp. 1-29, 2023.
[24] X. Xu, A. Collin, S. Z. Djokic, R. Langella, A. Testa, and J. Drapela, "Experimental evaluation and classification of LED lamps for typical residential applications," 2017 IEEE PES Innov. Smart Grid Technol. Conf. Eur. ISGT-Europe 2017 - Proc., vol. 2018-Janua, pp. 1-6, 2017.
[25] W. T. Tsai, Y. J. Chen, and Y. M. Chen, "A Modified Forward Forward PFC Converter for LED Lighting Applications," IEEE Open J. Power Electron. vol. 3, no. August, pp. 787-797, 2022.
[26] J. Hernandez, A. A. Romero, S. Muller, and J. Meyer, "Harmonic Distortion in Low Voltage Residential Grids Caused by LED Lamps," Proc. Int. Conf. Harmon. Qual. Power, ICHQP, vol. 2022-May, pp. 25-30, 2022.
[27] X. Liang, Y. Luy, and D. O. Koval, "Investigation of input harmonic distortions of variable frequency drives," Conf. Rec. - Ind. Commer. Power Syst. Tech. Conf., 2007.
[28] H. Soltani, F. Blaabjerg, F. Zare, and P. C. Loh, "Effects of Passive Components on the Input Current Interharmonics of Adjustable-Speed Drives," IEEE J. Emerg. Sel. Top. Power Electron. vol. 4, no. 1, pp. 152-161, 2016.
[29] R. Pandurangan, K. Palanisamy, and P. Shanmugam, "A comprehensive study of grid impedance and its reliability effects on variable frequency drive," Int. J. Power Electron. Drive Syst., vol. 14, no. 2, pp. 673-687, 2023.
[30] EN 50160, Ed., Standard EN 50160. Voltage characteristics of electricity supplied by public distribution systems. Brussels, Belgium: CENELEC, 2010.
[31] K. Sajjad, G. Kalsoom, and A. Mughal, "Simplified THD measurement and analysis for electronic power inverters," Proc. 2015 12th Int. Bhurban Conf. Appl. Sci. Technol. IBCAST 2015, pp. 186-191, 2015.
[32] M. H. J. H. Bollen and I. Y. H. Gu, Signal Processing of Power Quality Disturbances. Wiley-IEEE Press, 2006.
[33] M. S. S. S. M. Basir, R. C. Ismail, K. H. Yusof, N. I. A. Katim, M. N. M. Isa, and S. Z. M. Naziri, "An implementation of Short Time Fourier Transform for Harmonic Signal Detection," J. Phys. Conf. Ser. vol. 1755, no. 1, p. 12013, 2021.
[34] L. Alfieri, A. Bracale, and A. Larsson, New power quality indices for the assessment of waveform distortions from 0 to 150 kHz in power systems with renewable generation and modern non-linear loads, vol. 10, no. 10. 2017.
[35] X. Xu, A. J. Collin, S. Z. Djokic, R. Langella, and A. Testa, "Operating cycle performance, lost periodicity, and waveform distortion of switch-mode power supplies," IEEE Trans. Instrum. Meas. vol. 67, no. 10, pp. 2434-2443, 2018.
[36] X. Xiao, S. Djokic, R. Langella, and A. Testa, "Performance comparison of three main SMPS types under sinusoidal and distorted supply voltage," 2017 IEEE Manchester PowerTech, Powertech 2017, pp. 1-6, 2017.
[37] S. K. Jain and S. N. Singh, "Harmonics estimation in emerging power system: Key issues and challenges," Electr. Power Syst. Res. vol. 81, no. 9, pp. 1754-1766, 2011.
[38] P. F. Ribeiro, Time-Varying Waveform Distortions in Power Systems. New York, NY, USA: John Wiley & Sons, 2009.
[39] W. R. Oliveira, A. L. F. F. Filho, and J. Cormane, "A contribution for the measuring process of harmonics and interharmonics in electrical power systems with photovoltaic sources," Int. J. Electr. Power Energy Syst., vol. 104, no. July 2018, pp. 481-488, 2019.
[40] Union of the Electricity Industry Eurelectric, Ed., Application guide to the European Standard EN 50160 on "voltage characteristics of electricity supplied by public distribution systems". Electricity Product Characteristics and Electromagnetic Compatibility, no. July. 23002Ren9530: Ref, 1995.
[41] A. Arranz-Gimon, A. Zorita-Lamadrid, D. Morinigo-Sotelo, and O. Duque-Perez, "A Study of the effects of time aggregation and overlapping within the framework of IEC standards for the measurement of harmonics and interharmonics," Appl. Sci., vol. 9, no. 21, p. 4549, 2019.
[42] A. Arranz-Gimon, A. Zorita-Lamadrid, D. Morinigo-Sotelo, and O. Duque-Perez, "Analysis of the use of the Hanning Window for the measurement of interharmonic distortion caused by close tones in IEC standard framework," Electr. Power Syst. Res., vol. 206, p. 107833, May 2022.
[43] G. Anne, M. Jan, and R. Sarah, "Comparison of Measurement Methods for the Frequency Range 2-150 kHz (Supraharmonics)," 9th IEEE Int. Work. Appl. Meas. Power Syst. AMPS 2018 - Proc., pp. 1-6, 2018.
[44] M. Klatt, J. Meyer, and P. Schegner, "Comparison of measurement methods for the frequency range of 2 kHz to 150 kHz," Proc. Int. Conf. Harmon. Qual. Power, ICHQP, pp. 818-822, 2014.
[45] Z. An, T. Wang, Y. Wang, S. Tang, S. Tao, and Y. Xu, "A variable bandwidth method for supraharmonic band aggregation," Proc. 14th IEEE Conf. Ind. Electron. Appl. ICIEA 2019, pp. 1090-1094, 2019.
[46] Y. Wang, Y. Xu, S. Tao, A. Siddique, and X. Dong, "A Flexible Supraharmonic Group Method Based on Switching Frequency Identification," IEEE Access, vol. 8, pp. 39491-39501, 2020.
[47] T. M. H. H. Slangen, V. Ćuk, J. F. G. Cobben, and E. C. W. De Jong, "Variations in Supraharmonic Emission (2-150 kHz) of an EV Fast Charging Station under Different Supply- and Operating Conditions," IEEE Power Energy Soc. Gen. Meet. vol. 2023-July, pp. 1-5, 2023.

ANGEL ARRANZ-GIMON received the B.S. degree in telecommunications engineering, the M.S. degree in electronics engineering, and the Ph.D. degree in industrial engineering from the University of Valladolid (UVA), Valladolid, Spain, in 1991, 1999 and 2020, respectively. He has been with the Electronic Technology Department, UVA, since 1991, first as an Assistant Professor, and an Associate Professor since 1998, engaged in the development and design of analog and digital electronics systems. His research interests include digital signal processing, condition monitoring, and measurement and analysis of electric power quality.

DANIEL MORINIGO-SOTELO (M'04) received the B.S. and Ph.D. degrees in electrical engineering from the University of Valladolid (UVa), Spain, in 1999 and 2006, respectively. He was a research collaborator on Electromagnetic Processing of Materials with the Light Alloys Division of CIDAUT Foundation since 2000 until 2015. He is currently with the Research Group on Analysis and Diagnostics of Electrical Grids and Installations (ADIRE), that belongs to the ITAP Institute (UVA), and with the HSPdigital Research Group, Mexico. His current research interests include fault detection and diagnostics of induction machines, and power quality.

ANGEL ZORITA-LAMADRID received the B.S. degree in electric engineering, the M.S. degree in industrial engineering, and the Ph.D. degree in industrial engineering from the University of Valladolid (UVA), Valladolid, Spain, in 1990, 2001 and 2006, respectively. He has been professor in the Department of Electrical Engineering at the University of Valladolid since 1990. Member of the Research Group recognised by the University of Valladolid called ADIRE (Analysis and Diagnosis of Electrical Installations and Networks), and a member of the University Research Institute of the University of Valladolid called the Institute of Advanced Production Technologies.

His research interests include the analysis of the reliability and maintenance of electrical installations, measurement and analysis of the quality of electrical energy, electrical energy efficiency studies and characterisation and development of electrical demand models, and research in the field of management and control of electrical microgrids, fields in which he has participated in numerous projects and have published more than 70 articles in journals and conferences.

Angel Zorita-Lamadrid's awards and honours include the Thomas Hawskey Gold Medal awarded by the UK College of Mechanical Engineers, and the William Alexander Agnew Meritorious Award/Clarence Noel Goodall Award awarded by the Railway Division of the UK College of Mechanical Engineers.

Oscar Duque-Perez is an associate professor of Electrical Engineering at the University of Valladolid (UVa), Spain. He received his B.S. and Ph.D. from UVa, in 1992 and 2000, respectively. In 1994, he joined the Department of Electrical Engineering of the School of Industrial Engineering, UVa. He is a member of the research group on Analysis and Diagnostics of Electrical Grids and Installations (ADIRE) and ITAP, University of Valadolid. He has published over 100 journal and conference papers and has been collaborating in R+D Projects with Private Companies such as Iberdrola, Adif or Redalsa as well as R+D public funded projects for more than twenty years. Duque-Perez received the Thomas Hawskley Gold Medal from the Institution of Mechanical Engineers, UK and the William Alexander Agnew Meritorious Award/Clarence Noel Goodall Award from the Institution of Mechanical Engineers, Railway Division, UK. His main research fields are electric machines condition monitoring, power systems reliability and power quality, and electric energy efficiency.